Eur. Phys. J. B **4**, 313–319 (1998)

THE EUROPEAN PHYSICAL JOURNAL B

© EDP Sciences
Springer-Verlag 1998

Ascending air bubbles in protein solutions

C. Ybert[a] and J.-M. di Meglio

Institut Charles Sadron[b] and Université Louis Pasteur, 6 rue Boussingault, 67083 Strasbourg Cedex, France

Received: 6 March 1998 / Revised and accepted: 6 May 1998

Abstract. We report measurements of the ascending velocity of air bubbles in protein (bovine serum albumin) solutions. We show that, because of the protein molecules adsorbed on their surface, the terminal ascending velocity of bubbles is strongly reduced compared to the terminal velocity in pure water: protein-covered bubbles behave hydrodynamically as solid spheres. From the evolution of the ascending velocity with time, we can derive the amount of protein needed to immobilize the bubble interface which is $0.5\ \mathrm{mg\,m^{-2}}$, *i.e.* only one fifth of the amount adsorbed at equilibrium in the range of used bulk concentrations.

PACS. 68.10.Et Interface elasticity, viscosity, and viscoelasticity – 83.50.Lh Interfacial and free surface flows; slip – 82.70.y Disperse systems

1 Introduction

The stability of aqueous foams, *i.e.* a collection of air cells closed by water walls, is usually obtained through the addition of surfactants such as soap molecules or proteins which denaturate at interfaces to allow a microsegregation of the hydrophilic and the hydrophobic residues of their constitutive amino-acids. The stability does not originate from the drop of the interfacial tension caused by the surfactants adsorption but from the ability for the surfactant molecules to build surface tension gradients through concentration gradients. The associated surface stresses can then balance the weight of the films [1] or the viscous stresses associated to the drainage of the foam [2]. When an aqueous foam is made by bubbling a gas into a liquid, we might then like to know how much surface-active materials is collected along the path between the birth place of the bubble (capillary nozzle, sintered glass *etc.*) and the free surface of water. We present in this paper a study on the ascending velocity of air bubbles in protein solutions.

2 Experimental section

2.1 Materials

Bovine serum albumin (BSA) has been purchased from Sigma (purity > 97%, essentially fatty acid free grade) and used as received. Solutions were prepared with Milli-Q water; pH was about 5.5. All glassware was rinsed with ample amount of Milli-Q water before use. Experiments have been all performed at room temperature $(20 \pm 2)°\mathrm{C}$.

[a] e-mail: ybert@ics.u-strasbg.fr
[b] Unité Propre de Recherche du CNRS (UPR022).

2.2 Experimental setup

Experiments were performed in a glass cylinder of 6 cm diameter and 24 cm height. Air bubbles are generated one by one at the extremity of a L-shaped glass capillary tube using a 2 ml syringe (Fig. 1). The characteristic time of formation of a bubble is about 0.2 s. The image of a rising bubble is captured by a CCD video camera (Micam VHR 1000, Computar Zoom 12.5–75 mm) connected to a Super VHS JVC video recorder. Each image is digitised with a PC frame grabber board (Data Translation DT55). The bubble velocity U as a function of the travelled distance h is calculated from the succession of the bubble positions, as the mean value of the left and the right derivative

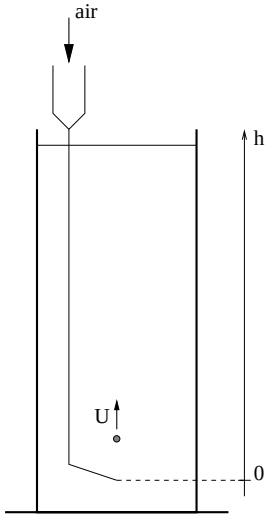

Fig. 1. Experimental setup.

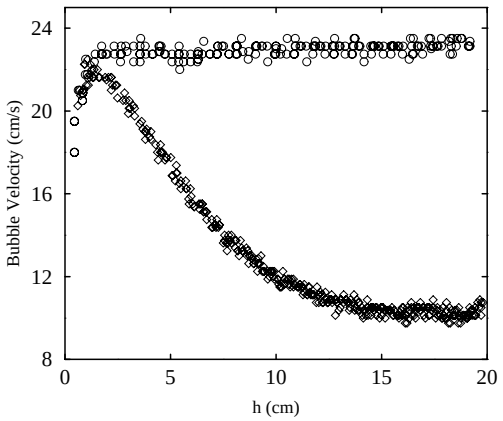

Fig. 2. Evolution of the bubble velocity with h, $R = 0.43$ mm; (○) pure water, (◇) BSA solution $c = 10$ mg/l.

(except for the first point of course, where only the right derivative can be defined).

The video camera acquires 25 images per second with a spatial resolution of 0.25 mm per pixel of the CCD-sensitive device. The resulting error on the bubble velocity is about 0.3 cm/s. To improve the sampling on h, experimental results for $U(h)$ are made from the superimposition of data from at least 10 different bubbles.

In order to measure the bubble radii, the zoom lens of the camera is replaced by a binocular microscope (Olympus SZ11). In this configuration a pixel corresponds to 5 μm. The size was measured once for each capillary tube and supposed to remain constant thereafter. This assumption is well-supported by the excellent reproducibility of the results.

3 Results and discussion

3.1 General Description of U(h)

3.1.1 Pure water

For an air bubble in pure water (Fig. 2), the motion exhibits two different regimes: an inertial regime where the bubble is accelerating, followed by a stationary regime when buoyancy and drag forces balance each other. The final value of the bubble velocity in a pure liquid U_0 at moderate Reynolds numbers – from 70 to 300 in our experiments – has been first calculated, neglecting the shape deformation, by Levich [3] and then refined by Moore [4] who obtained

$$U_0 = \frac{gR^2}{9\nu}\left(1 - \frac{2.11}{\sqrt{Re}}\right)^{-1} \quad (1)$$

with R the bubble radius, ν the kinematic viscosity of water, g the acceleration of gravity and Re the Reynolds number:

$$Re = \frac{2RU_0}{\nu}. \quad (2)$$

The experimental and theoretical terminal velocities in water are in good agreement indicating that our water is free from impurities.

Strictly speaking, the bubble velocity on the final plateau should increase during the ascension due to the change of the hydrostatic pressure. Neglecting the correction term in $\sqrt{Re}$ in equation (1), the slope of the plateau is given by

$$\frac{dU}{dh} \simeq \frac{2}{3}\frac{\rho g}{P_0}U \quad (3)$$

where P_0 is the atmospheric pressure and ρ the volumic mass of water. For a 20 cm rise with a mean velocity of 20 cm/s, this leads to an increase of 0.3 cm/s in U_0. Velocities between the beginning and the end of the plateau do seem to increase by such a quantity, however nothing definitive can be said as it is very close to the noise of measurement.

3.1.2 Protein solution

The same evolution of U during the rise of the bubble is plotted in Figure 2 for a solution of 10 mg/l of BSA. Contrary to the pure water case, it is possible to distinguish 3 different regimes for the bubble motion in presence of BSA. First the inertial phase, which remains unaffected compared to the pure liquid case, at the end of which the velocity passes through a maximum U_M. Then, in a second regime, the bubble is slowing down while rising: we believe this to occur through a quasistationary process during which buoyancy always equilibrates drag force which is continuously increasing. Finally a stationary state is reached corresponding to a constant velocity well below U_0.

Following Aybers and Tapuccu [5] who have reported a slowing down of bubbles in distilled water due to accumulation of impurities, we attribute the velocity decrease occurring in the second regime to an increase in the protein surface concentration Γ on the bubble. Adsorption of proteins affects the velocity through the Marangoni effect: the external flow creates an accumulation of protein at the rear part of the bubble which is responsible for a surface tension gradient along the interface. This gradient induces a surface stress which opposes the flow: the fluid velocity in the vicinity of the surface is decreased compared to the pure liquid case. Velocity gradients, and consequently viscous dissipation, are therefore enhanced which leads to a lower rising speed.

In this description, the maximum is the first point for which drag and gravity are equal: U_M is thus dependent on the total amount of protein collected during the first regime of acceleration. If this quantity is small, the drag force at the end of the inertial regime is almost identical to the one for pure liquid and $U_M = U_0$ as in Figure 2.

3.2 Final stationary state

Marangoni effect reduces the fluid velocity close to the surface, decreasing the so-called surface mobility (such an

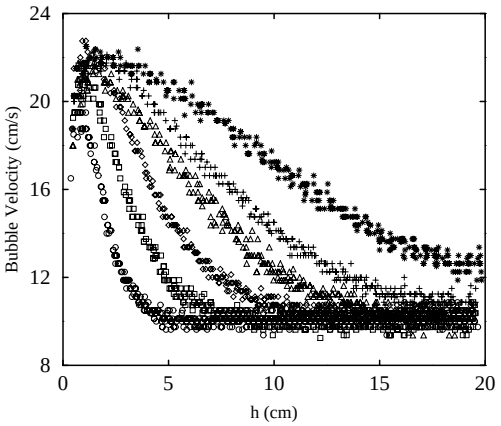

Fig. 3. Influence of the BSA concentration on $U(h)$, $R = 0.43$ mm; (○) 40 mg/l, (□) 20 mg/l, (◇) 14.5 mg/l, (△) 7.5 mg/l, (+) 6.25 mg/l, (∗) 5 mg/l.

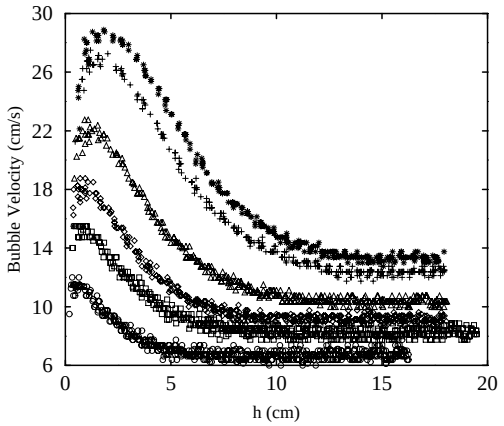

Fig. 4. $U(h)$ in BSA solution ($c = 14.5$ mg/l) for different bubble diameters: (○) 0.59 mm, (□) 0.71 mm, (◇) 0.79 mm, (△) 0.86 mm, (+) 0.97 mm, (∗) 1.08 mm.

effect of interface rigidification has already been visualised for drops and surfactants [6,7]). The limit of this phenomenon is reached when the surface has lost all of its mobility then imposing a zero velocity boundary condition for the external fluid. In such a situation, the bubble is hydrodynamically equivalent to a rigid sphere of same density and same diameter.

Figure 3 shows the influence of the protein concentration on $U(h)$. A detailed study of those results will be done in a next section but we can note at this point that the bubble velocity reaches the same stationary value for all tested BSA concentrations c. This final regime, common to a whole range of concentrations, is very likely to be the ultimate state of immobilisation, namely the rigid surface. The detachment of the boundary layer occurring for $Re > 20$ with solid spheres has mainly restricted the studies to experimental and numerical investigations. However the relation between Re and the drag coefficient C_D, where C_D is related to the drag force F_D by $F_D = (\pi R^2)\rho U^2 C_D/2$ is well-known.

Figure 4 shows $U(h)$ for different bubble radii. From the terminal velocity found for each R, it is possible to calculate Re in this final state. Balancing buoyancy and drag forces allows the experimental determination of C_D through the expression

$$C_D = \frac{8}{3}\frac{Rg}{U^2}. \tag{4}$$

We have plotted in Figure 5 the experimental $C_D(Re)$ relation for the bubble final state and compared it to an empirical relation for a solid sphere [8] and to numerical simulations for solid sphere [9]. The correspondence between data from bubbles and solid spheres predictions is very good thus establishing the rigid character of the bubble surface in the terminal stationary regime of the bubble rise.

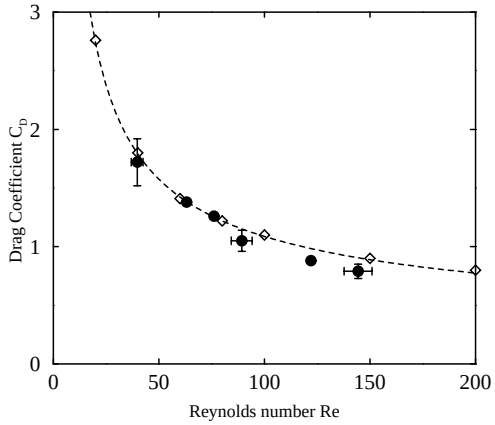

Fig. 5. Drag coefficient as a function of Reynolds number: (•) experimental results for bubbles (terminal velocity), (−−) empirical relation for solid spheres (Clift, Grace and Weber), (◇) numerical simulation for solid spheres (Rimon and Cheng).

3.3 Experimental measurement of U(Γ)

3.3.1 Is U only a function of Γ?

Proteins on the bubble interface are modifying the hydrodynamical boundary condition and therefore the bubble velocity. However for $U(h)$ to be a function of the sole variable Γ two points have to be satisfied. First there should be no effects of film reorganisation on the time scale of the velocity evolution: this assumes that no individual molecular denaturation and no global rearrangement of the layer on the surface should occur. Second, there must be no inertial effects which restricts, at least, the analysis to the velocity evolution after the maximum. Also in this second regime, the quasistationarity assumption has to be proved.

To investigate furthermore the latter points, we have modified the original experiment. A second capillary tube,

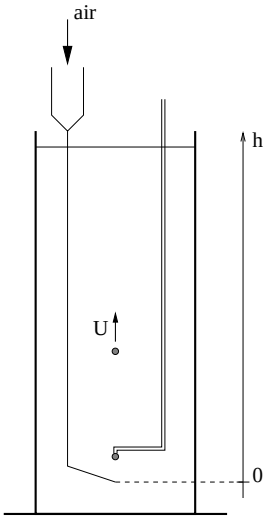

Fig. 6. Derivation of the experimental setup allowing bubble pre-load.

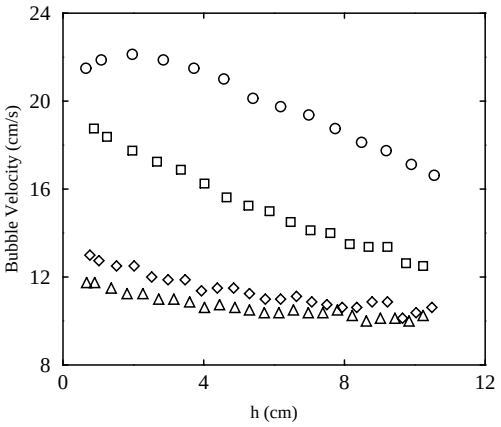

Fig. 7. $U(h)$ evolution for different incubation times, R = 0.43 mm, c = 5 mg/l; (○) t_{inc} = 0 s, (□) t_{inc} = 8 s, (◇) t_{inc} = 36 s, (△) t_{inc} = 61 s.

a few millimetres above the first one, is added to the experimental setup Figure 6. The bubble is generated as previously with the first L-shaped capillary tube, immediately released and captured by the second one. It is kept at rest for an incubation time t_{inc} during which proteins adsorb at the interface. At the end of this incubation period, the bubble is released and starts its rise. We study the influence of the initial surface concentration Γ_0, function of t_{inc}, on $U(h)$.

$U(h)$ is plotted in Figure 7 for 4 different incubation times t_{inc}, corresponding to 4 different initial surface concentrations Γ_0. If U were only a function of Γ it should be possible to reconstruct the whole evolution as shown in Figure 2 from the superimposition of the data for different t_{inc}, just changing the height origin to take into account the different Γ_0. Figure 8 presents the 4 previous sets of data translated along h and shows how it compares with the whole $U(h)$ evolution obtained from a single bubble without protein pre-load. The matching between the two evolutions is excellent furnishing evidence that the slowing down of the bubble is due to a continuous increase in Γ, the velocity adjusting itself "instantaneously" to the resulting change in the drag force.

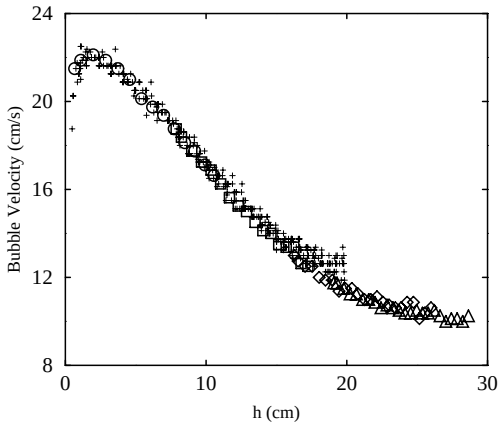

Fig. 8. Reconstitution of the total $U(h)$ relation from the translation of the data from different incubation times, R = 0.43 mm, c = 5 mg/l; (+) complete $U(h)$ evolution without pre-load, (○) t_{inc} = 0 s, (□) t_{inc} = 8 s, (◇) t_{inc} = 36 s, (△) t_{inc} = 61 s.

From Figure 7, we see that U_M, corresponding to the first point at which buoyancy and drag forces equilibrate, is a function of t_{inc} and thus of Γ_0. If we neglect the adsorbed amount during the inertial stage, which appears to be legitimate for the studied bulk concentration since $U_M = U_0$ for $t_{inc} = 0$, the measurement of $U_M(\Gamma_0)$ is a measurement of the expected $U(\Gamma)$ relation.

3.3.2 Measurement of U(Γ)

Figure 9 reports U_M as a function of the incubation time t_{inc}. To relate t_{inc} to the the initial surface concentration Γ_0, a modelisation is needed. While kept at rest at the extremity of the hanging capillary protein adsorption to the bubble occurs in the classical way: from an infinite quiescent solution. In such a situation, we have shown [10] that for surface pressures below 10 mN/m, the adsorption kinetics is controlled by transport from the bulk. For time t below 10 minutes natural convection in the quiescent liquid is negligible and the surface concentration is given by a simple diffusion law [11]

$$\Gamma_0(t_{inc}) = 2c\sqrt{\frac{Dt_{inc}}{\pi}} \tag{5}$$

with D the lateral diffusion coefficient of BSA ($D = 6.7 \times 10^{-11}$ m^2/s [12]). Data for $U_M(t_{inc})$ can therefore be plotted as a function of Γ_0 (Fig. 10). Notice the collapse of the results obtained with 3 different concentrations indicating the validity of the model expression for $\Gamma_0(t_{inc})$. This provides, to our knowledge, the first experimental determination of the relation $U(\Gamma)$ between bubble velocity and surface coverage.

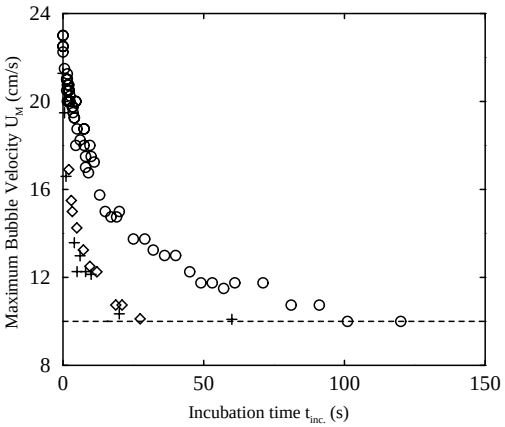

Fig. 9. Evolution of the maximum bubble velocity with the incubation time, $R = 0.43$ mm; $(--)$ solid sphere limit, $(\circ)$ $c = 5$ mg/l, $(\diamond)$ $c = 10$ mg/l, $(+)$ $c = 13$ mg/l.

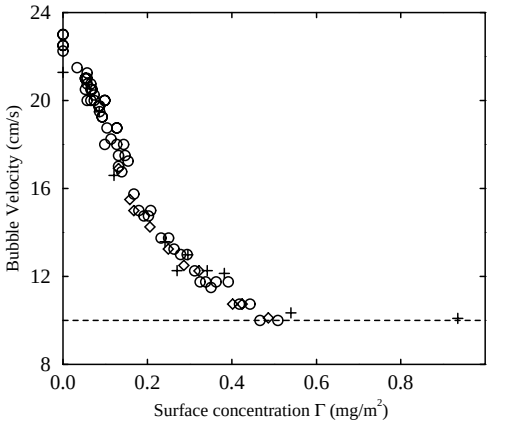

Fig. 10. Relationship between U and Γ, $R = 0.43$ mm; $(--)$ solid sphere limit, $(\circ)$ $c = 5$ mg/l, $(\diamond)$ $c = 10$ mg/l, $(+)$ $c = 13$ mg/l.

The minimum amount of protein needed to completely immobilise the interface is 0.5 mg/m^2. This is in agreement with a simple estimation consisting in the equilibration of the viscous stress by the surface tension gradient along the interface:

$$\frac{\Delta\gamma}{R} \simeq \eta\frac{U}{R} \qquad (6)$$

where $\Delta\gamma$ is the surface tension difference between the front and the rear part of the bubble and η is the fluid viscosity. With U around 10 cm/s, $\Delta\gamma \simeq 0.1$ mN/m which indicates that the mean surface concentration on the bubble is about 0.4 mg/m^2. From simulations by McLaughlin [13] that give the surface tension gradient along the interface, it is possible to estimate the minimum amount of proteins on the bubble able to generate this gradient. We found a minimum mean BSA surface concentration on the bubble for rigidifying the surface of $\Gamma_{min} \simeq 0.8$ mg/m^2 for a 1 mm diameter bubble. This is an upper bound for us as experiments were performed with 0.86 mm diameter bubbles: using equation (6) and considering the bubble velocity behaves as R^2, an estimation of the correction due to the diameter difference is obtained. The resulting minimum surface concentration in our system, evaluated from the simulations, is $\Gamma_{min} \simeq 0.6$ mg/m^2 which shows a very good agreement with experiments.

An interesting point is that for such a low surface concentration, proteins are, without any external flow, in a gaseous state. The typical equilibrium surface concentration for the studied concentration range is between 2 and 3 mg/m^2 as determined by Graham and Phillips [14], *i.e.* a significant higher concentration. This very dilute surface state is nevertheless able to rigidify the interface during the bubble ascension.

3.4 Influence of the protein concentration on U(h)

We have shown in the previous section that the bubble velocity is just a function of the protein surface concentration. This surface concentration evolves during the rise through the protein flux created, in particular, by the external flow. We try in this section to characterise this protein flux through its protein bulk concentration dependency, for a fixed bubble radius R.

From Figure 3 where $U(h)$ is plotted for 6 different concentrations, it is possible to extract a few general trends: the higher the concentration c, the lower the maximum velocity U_M and the faster the decrease toward the final velocity. We have already noticed, in addition, that over the whole studied decade in c, U converges toward the same final stationary regime, namely the rigid surface regime.

Increasing c enhances the protein flux toward the interface. The adsorption during the inertial regime, neglected up to now, can lead at high concentrations to an amount of protein at the end of this regime high enough to significantly modify the drag force. Consequently, the velocity at which the quasistationary state is reached is lowered. The same increase of the protein flux explains that Γ is increasing faster at high concentration thus leading to faster velocity decrease with h.

As already mentioned the BSA adsorption kinetics on immobile bubbles is governed by transport from the bulk, namely convection and diffusion, for moderate surface pressures [10]. However contrary to the motionless problem, the determination of this transport is rather complicated for an ascending bubble since the hydrodynamics is not analytically soluble at intermediate Reynolds numbers. It is nevertheless possible to obtain, in the case of a bubble with a fully mobile interface (thus restricting the validity to the very initial stage of the motion) an expression for this flux with a simple argument; we retrieve in that way results from Levich calculations [3] at low Reynolds or from Yang *et al.* [15] at large Reynolds. The adsorption is supposed to occur through diffusion, the role of convection being in a constant renewal of the fluid surrounding the bubble. The time τ for this renewal is about

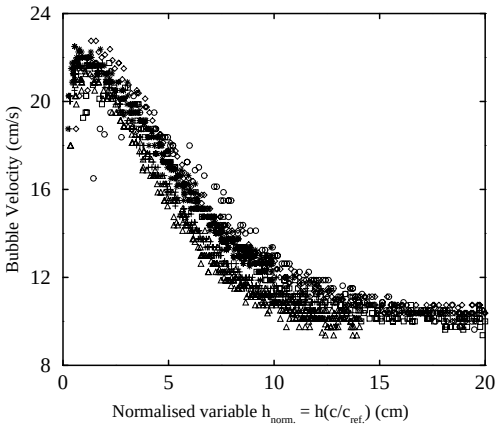

Fig. 11. Rescaled data with respect to concentration, $R = 0.43$ mm and $c_{ref} = 10$ mg/l; (○) 40 mg/l, (□) 20 mg/l, (◇) 14.5 mg/l, (△) 7.5 mg/l, (+) 6.25 mg/l, (∗) 5 mg/l.

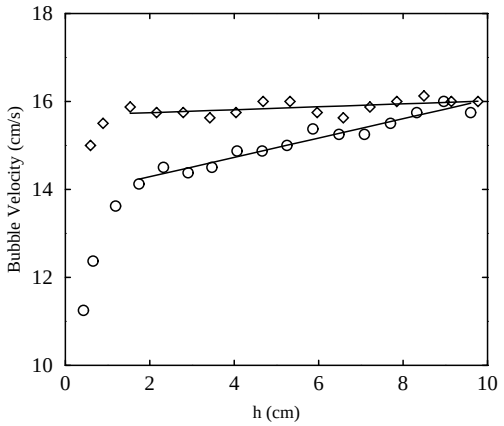

Fig. 12. Comparison of $U(h)$ for pre-loaded bubbles rising in pure water, $R = 0.43$ mm. (—) linear regressions, (○) SDS pre-loaded in $c = 1$ mg/l, (◇) BSA pre-loaded in $c = 10$ mg/l.

the time for the bubble to move by its size

$$\tau \simeq \frac{R}{U}. \tag{7}$$

During such a period, adsorption occurs through diffusion

$$\Delta\Gamma \simeq c\sqrt{D\tau} \tag{8}$$

and the protein flux to the interface can finally be estimated by

$$\frac{d\Gamma}{dt} \simeq \frac{\Delta\Gamma}{\tau} = c\sqrt{\frac{DU}{R}}. \tag{9}$$

Once a stagnant cap has formed at the rear pole of the bubble, a turbulent wake appears and this estimation no longer holds. It is nevertheless possible to suppose that the flux will remain of the form

$$\frac{d\Gamma}{dh} = c\, f(D, R, U). \tag{10}$$

In the region where U is a function of the sole variable Γ (slowing down regime), equation (10) implies

$$\frac{dU}{dh} = c\, g(D, R, U). \tag{11}$$

From this last relation it follows that the slowing down part of the different $U(h)$ plots Figure 3 should collapse on a master curve when plotted as a function of the normalised variable $h_{norm} = h(c/c_{ref})$, with c_{ref} an arbitrary reference concentration. Except for the inertial stage which is beyond the scope of this rescaling, this master curve clearly exists as shown in Figure 11 where the 6 different concentrations measurements collapse on the same $U(h_{norm})$ curve.

3.5 Comparison between BSA and SDS

On the whole concentration decade presently studied bubbles achieve a completely immobile surface: this is qualitatively different from existing results for usual surfactants as soap molecules. For those systems, Duineveld [16] or Griffith [17] have shown that the terminal velocity of an ascending bubble is a function of the surfactant concentration up to a critical c at which the complete surface immobilisation is achieved. Above that concentration the terminal velocity is equal to the velocity U_S of the equivalent solid sphere.

The surfactant behaviour is explained by an equilibrium between the bulk and the surface that fixes the amount of surfactant on the bubble surface for a given c. This is not likely to occur with proteins where desorption is very slow and for which the question of adsorption reversibility is frequently questioned. We have therefore looked at the desorption behaviour of both SDS and BSA through a simple derivation of our experiment.

We use the same system than for measuring $U(\Gamma)$ but this time the glass cylinder is filled with Milli-Q water whereas the hanging capillary contains a solution of either SDS or BSA. The bubble is generated as usual and captured by the hanging capillary. It is there in contact with the solution containing one of the two tensio-active substances which then adsorbs at the interface. This preloaded bubble is released and rises in pure water. Figure 12 compares the evolution of U for two bubbles, one preloaded with BSA, the other pre-loaded with SDS. Both bubbles are starting with intermediate surface mobility (U is between U_S and U_0) but whereas U remains constant for BSA (the slope of the linear regression is due to hydrostatic pressure change), the SDS bubble accelerates. This behaviour clearly indicates that a substantial desorption exists, leading to a remobilisation of the interface. For the experimented time scales, BSA appears irreversibly adsorbed and even if experiments could not be performed for lower concentrations due to the limited height of our cylinder we believe that even for small c, BSA accumulates on the interface and achieves its complete immobilisation after a finite h.

4 Conclusion

We have presented a study of the velocity of rising bubbles in protein solutions. We have shown that the velocity of the bubbles, after a first inertial regime, decreases to reach a terminal velocity equal to about half the terminal velocity of bubbles of the same size in pure water: this is due to the adsorption of proteins that progressively modifies the hydrodynamic boundary conditions from a stress-free to a rigid surface. Moreover, we have proved that this adsorption is irreversible and that only a small fraction of the equilibrium adsorbed amount is necessary to rigidify the interface.

We thank the beverage division of Danone for supporting our research.

References

1. P.-G. de Gennes, C. R. Acad. Sci. Paris, Série II **305**, 9 (1987).
2. J. Lucassen, in *Anionic Surfactants*, edited by J. Lucassen-Reynders (Marcel Dekker, New York, 1981), Chap. 5.
3. V.G. Levich, *Physicochemical Hydrodynamics* (Prentice Hall, New Jersey, 1962).
4. D.W. Moore, J. Fluid Mech. **16**, 161 (1963).
5. N.M. Aybers, A. Tapucu, Wärme- und Stoffübertragung **2**, 118 (1969).
6. T.J. Horton, T.R. Fritsch, R.C. Kintner, Can. J. Chem. Eng. **43**, 143 (1965).
7. F.H. Garner, A.H.P. Skelland, Chem. Eng. Sci. **4**, 149 (1955).
8. R. Clift, J.R. Grace, M.E. Weber, *Bubbles, drops and particles* (Academic Press, new York, 1978).
9. Y. Rimon, S.I. Cheng, Phys. Fluids **12**, 949 (1969).
10. C. Ybert, J.-M. di Meglio, Langmuir **14**, 471 (1998).
11. A.F.H. Ward, L. Tordai, J. Chem. Phys. **14**, 453 (1946).
12. J.J.S. Shen, R.F. Probstein, Ind. Eng. Chem. Fundam. **16**, 459 (1977).
13. J.B. McLaughlin, J. Colloid Interf. Sci. **184**, 614 (1996).
14. D.E. Graham, M.C. Phillips, J. Colloid Interf. Sci. **70**, 415 (1979).
15. S.-M. Yang, S.P. Han, J.J. Hong, J. Colloid Interf. Sci. **169**, 125 (1995).
16. P.C. Duineveld, Ph.D. thesis, University of Twente (1994).
17. R.M. Griffith, Chem. Eng. Sci. **17**, 1057 (1962).